African Journal of Biotechnology Vol. 11(14), pp. 3250-3258, 16 February, 2012
Available online at http://www.academicjournals.org/AJB
DOI: 10.5897/AJB10.2422
ISSN 1684–5315 © 2012 Academic Journals

Full Length Research Paper

Load modeling for sharp V-cutter cutting litchi (*Litchi chinensis* Sonn.) stalk

Tian-hu Liu

College of Engineering, South China Agricultural University, Guangzhou, China.
E-mail: liuparalake@126.com. Tel: +86-13760863320. Fax: +86-20-85280783.

Accepted 19 September, 2011

Integrating picking institutions with autocontrol method led to the development of a new innovative 'hand-held auto-picker' for litchi (*Litchi chinensis* Sonn.) harvesting. Cutting load is a key parameter for 'hand-held auto-picker' operation. However, there is still no suitable model for cutting load setting. Hence, a model describing the relationship among cutting load, blade angle and friction coefficient was developed for cutting operation by sharp V-cutters. The model was based on analysis of mechanics of materials. A testing-equipment was developed and a series of tests was designed to verify such model. Results indicate that the cutting force trend-line calculated by the model is very similar to test results, but the calculated trend-line is much smoother. When radius of sample is between 5 and 7 mm, the calculated results were very approximate to the average of test results.

Key words: Litchi, picking, cutting force, model.

INTRODUCTION

Litchi (*Litchi chinensis* Sonn.) is an important economic fruit in Guangdong and Guangxi, China. At present, all of the picking (cut-off) work for litchi must rely on manual. Integrating picking institutions with autocontrol method led to the development of a new innovative 'hand-held auto-picker' for litchi harvesting. The harvesting method of litchi is different from that of apple, citrus and olive, in which the fruit stalks must be cut down from the trees by a pair of cutters. The goal of the current work was to develop a model describing the relationship among cutting load, blade angle and friction coefficient.

Studies about cutting have been conducted for crop plants such as oil palm (Razak, 1997), sugarcane (Liu et al., 2007), sesame stalk (Deniz et al., 2009), soya bean stalk (Mesquita and Hanna, 1995), cotton stalk (El Hag, 1971), pyrethrum flowers (Khazaei et al., 2002), alfalfa (Galedar et al., 2008) and sunflower (Kocabiyik and Kayisoglu, 2004). However, no reports on cutting litchi stalks have been published so far. The physical properties of litchi stalks are quite different from that of sesame stalks, soya bean stalks, cotton stalks, pyrethrum flowers, alfalfa and sunflower, etc. Cutting methods are also not the same; litchi stalks is cut using two opposed elements, but most of other plants are cut using single element. Cutting using single element differs greatly from cutting using two opposed elements (Yiljep and Mohammed, 2005). Cutting with single element can be referred to as pure impact cutting. Cutting using two opposed elements is cutting with counter-edge and thus, a counter-edge is used to provide the reaction force.

Xiao (2000) introduced a cutting force equation for wood machinery manufacturing, but such equation was based on several hypotheses. For example, it assumed that the specimen is a semi-infinite beam. Persson (1987) reviewed several studies on the cutting speed and concluded that cutting power is only slightly affected by cutting speed. More also, Tabatabaekoloor (2008) designed a pendulum type impact shear test apparatus to measure the energy required for cutting paddy stem and to determine the optimum values of blade bevel angle, oblique angle, tilt angle and blade cutting velocity for cutting paddy stem of Iranian "Sepidrood" variety. He found that blade bevel angle of 28°, oblique angle of 30°, tilt angle of 35° and blade velocity of 2.24 m/s are a

Figure 1. (a) Good cut kerf; (b) and (c) lacerated cut kerfs

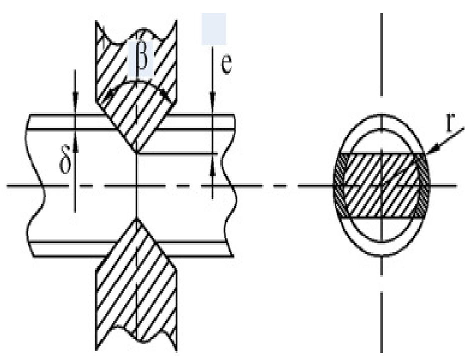

Figure 2. Relative position of cutter and stalk.

optimum. In addition, Majumdar and Dutta (1982) studied the required shearing energy for two varieties of rice and significant. Esehaghbeygi et al. (2009) also measured the shearing stress of wheat stalk and found that the blade oblique angle of 30° showed the least shearing stress.

Our previous studies indicated that cutting load is a very important parameter for litchi harvesting. Too low a cutting load will lead to incomplete cutting, and will further result in lacerated kerfs. Figure 1 shows some type of stalk kerfs. A lacerated kerf will destroy the fruit and the tree.

MODEL DEVELOPMENT

In the process of litchi picking, V-cutter cuts and squeezes into material from both sides of the stalk. Relative position of the cutter and the stalk is as shown in Figure 2, where δ is thickness of stalk skin, r is the radius of stalk, β is the blade angle or kerf angle and e is cutting depth. Axial sub-variety of wheat and they found that the effects of crop

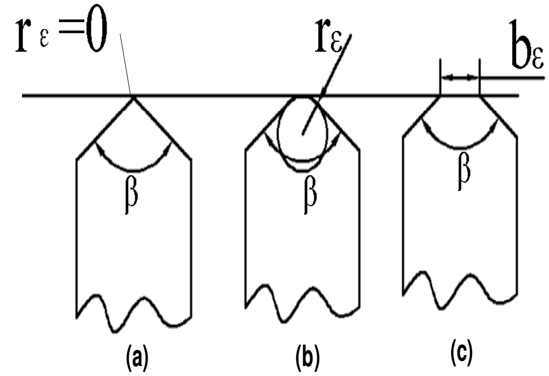

Figure 3. The shape of cut edge

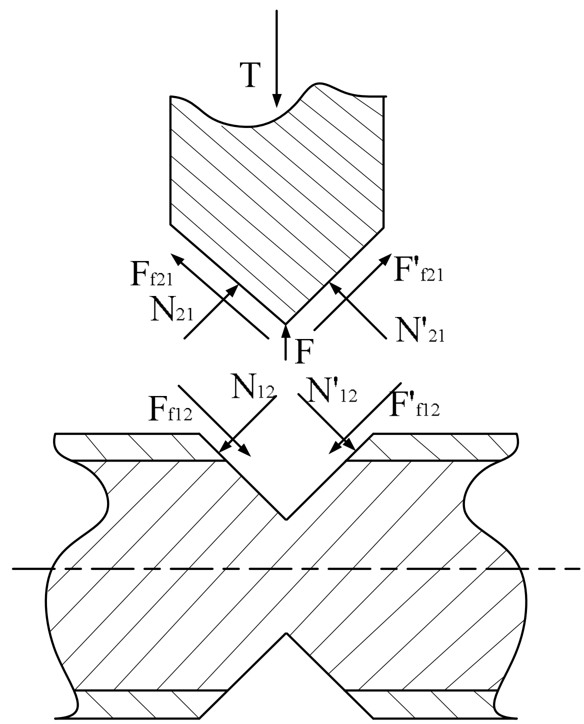

Figure 4. Interaction model between stalk and cutter.

type and edge angles on shearing energy were vector of the load on the back of cuter is stretch load acting on the stalk. For a newly grinded cutter, the width or radius of blade edge approaches zero, as shown in Figure 3a. When the cutter becomes wear and tear, there will be some arcs (Figure 3b) or small planes (Figure 3c) on the blade's edge. The interaction model between the stalk and the cutter is shown in Figure 4. Symbols and their indication are shown in Table 1.

Assumptions

The following assumptions were made:

Table1. Symbols and their indication.

Symbol	Indication
T	Pressure on the cutter
F	Effective cutting force
F_{f21} , F'_{f21}	Frictions
F_{f12} , F'_{f12}	Reactions of F_{f21} and F'_{f21}
N_{21}, N'_{21}	Pressure on the cutter blade
N_{12}, N'_{12}	Reactions of N_{21} and N'_{21}

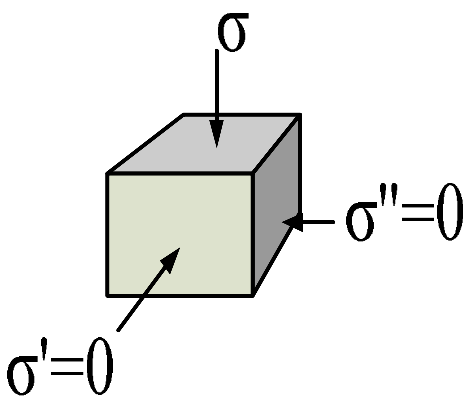

Figure 5. Stress state.

(a) Stalk material is anisotropy; its yield stress is angle-and direction-dependent.
(b) The blade edge is perpendicular to the center line of the litchi stalk.
(c) Cutters are very sharp, the width or radius of the blade edge equal to zero.

Cut force model

In structures that are anchored so as to prevent motion, there is obviously no acceleration and the forces must sum up to zero (Murray, 1982). In this case we have:

$$\vec{T}+\vec{F}+\vec{F}_{f_{21}}+\vec{N}_{21}+\vec{F}'_{f_{21}}+\vec{N}'_{21}=0 \quad (1)$$

The effective cutting force applied on the stalk is obtained and expressed as:

$$\vec{F}=-(\vec{T}+\vec{F}_{f_{21}}+\vec{N}_{21}+\vec{F}'_{f_{21}}+\vec{N}'_{21}) \quad (2)$$

The stresses σ of the materials touching with blade edge (Figure 5) is;

$$\sigma=\frac{F}{r_{\varepsilon}\times\bar{L}} \quad (3)$$

Where, $\bar{L}$ is the cutting length of blade.

Stage 0: The cutter moves forward until it touches with the stalk. e = 0, F = 0, $\sigma=0$.
Stage 1: The cutter starts touching with the stalk, e→0.

$\vec{F}_{f_{21}}\to 0$, $\vec{N}_{21}\to 0$, $\vec{F}_{f_{21}}\to 0$ and $\vec{N}'_{21}\to 0$.
Therefore, $\vec{T}=-\vec{F}$ and $\bar{L}\to 0$. At this moment, if $\vec{F}>0$, then the stress approach infinite.

$$\sigma=\frac{T}{r_{\varepsilon}\times\bar{L}}\to\infty \quad (4)$$

According to strength theory, we might expect material to yield when $\sigma_{ri}\geq[\sigma]$. Accordingly, the following conclusions can be drawn: when the cut depth approach zero, as long as $\vec{T}>0$, the stalk material will be broken.
Stage 2: Further cutting until the stalk was cut off e >0. $\vec{F}_{f_{21}}>0$, $\vec{N}_{21}>0$, $\vec{F}'_{f_{21}}>0$, $\vec{N}'_{21}>0$, $\bar{L}>0$ and $r_{\varepsilon}=0$. At this state, the forces must also sum to zero:

$$\vec{T}+\vec{F}+\vec{F}_{f_{21}}+\vec{N}_{21}+\vec{F}'_{f_{21}}+\vec{N}'_{21}=0.$$

In addition to positive pressure, fiction is also acted on the contact face of the blade flank and the materials. The horizontal and vertical nodal forces are shown in Figure 6; these can be written as

$$\vec{N}_{12}=\vec{N}_{x12}+\vec{N}_{y12} \quad (5)$$

$$N_{x12}(\beta)=N_{12}(\beta)\cos\frac{\beta}{2},\quad N_{y12}(\beta)=N_{12}(\beta)\sin\frac{\beta}{2}$$

$$\vec{f}_{12}=\vec{f}_{x12}+\vec{f}_{y12} \quad (6)$$

$$f_{x12}(\beta)=f_{12}(\beta)\cos\frac{\beta}{2},\quad f_{y12}(\beta)=f_{12}(\beta)\sin\frac{\beta}{2}$$

These forces can be simplified to a slender bar subjected to an axial loading and a press, as shown in Figure 7. These loads can also be written as;

$$\vec{P}_1=\vec{N}_{x12}+\vec{f}_{x12},\quad \vec{P}_2=\vec{N}_{y12}+\vec{f}_{y12}$$

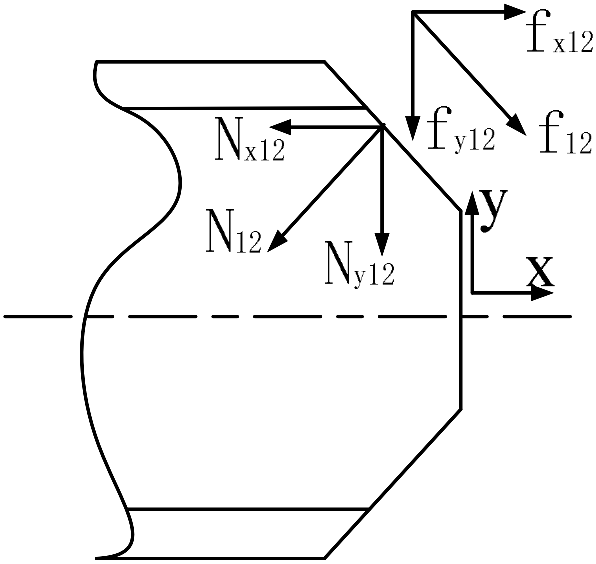

Figure 6. Load of local materials.

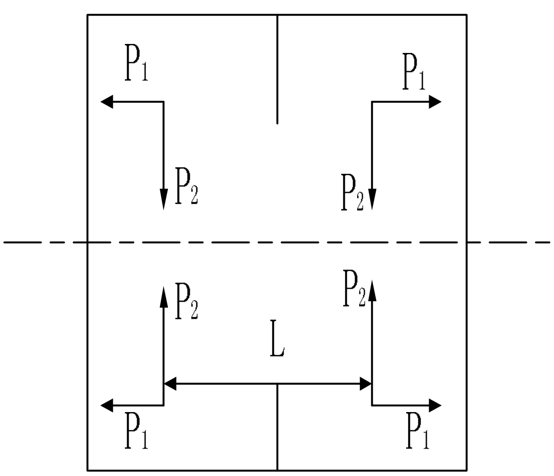

Figure 7. Simplified force model.

Magnitude of $\vec{P}_1$ is

$$P_1 = N_{x12}(\beta) - f_{x12}(\beta) = N_{12}(\beta)\sin\frac{\beta}{2} - f_{12}(\beta)\sin\frac{\beta}{2} \quad (7)$$

Magnitude of $\vec{P}_2$ is

$$P_2 = N_{y12}(\beta) - f_{y12}(\beta) = N_{12}(\beta)\cos\frac{\beta}{2} - f_{12}(\beta)\cos\frac{\beta}{2} \quad (8)$$

Referring to Figure 2, dangerous section is across blade edge and sum area of dangerous section is:

$$S(e) = 2\int_0^{r-e} 2\sqrt{r^2 - y^2}\,dy \quad (9)$$

$$= \pi r^2 - 2[r^2 \arccos\frac{r-e}{r} - (r-e)r\sin(\arccos\frac{r-e}{r})]$$

Dangerous section has two parts: the core and the bark. The area of core is

$$\begin{cases} S_1(e) = \pi(r-\delta)^2 & e \le \delta \\ S_1(e) = 2\int_0^{r-e} 2\sqrt{(r-\delta)^2 - y^2}\,dy & e > \delta \end{cases} \quad (10)$$

$$= \pi(r-\delta)^2 - 2[(r-\delta)^2 \arccos\frac{r-e}{r-\delta} - (r-e)(r-\delta)\sin(\arccos\frac{r-e}{r-\delta})]$$

While the area of bark is

$$\begin{cases} S_2(e) = S(e) - \pi(r-\delta)^2 - 2\int_{r-e}^{r} 2\sqrt{r^2 - y^2}\,dy & e \le \delta \\ S_2(e) = S(e) - S_1(e) & e > \delta \end{cases} \quad (11)$$

The strains of core material and bark material in the fiber direction can be written as ε1= ε2 = ε. The strains must also satisfy equilibrium equation, which can be written as:

$$S_1(e)\times E_1 \times \varepsilon + [S(e) - S_1(e)]\times E_2 \times \varepsilon = 2P_1$$

Where, E_1 is the elastic modulus of core material and E_2 is the elastic modulus of bark material.
This can also be written as;

$$\varepsilon = 2P_1 / \{S_1(e)\times E_1 + [S(e) - S_1(e)]\times E_2\} \quad (12)$$

The tensile stress, which core material withstands in the fiber direction, is

$$\sigma_1 = \varepsilon \times E_1 = 2P_1 \times E_1 / \{S_1(e)\times E_1 + [S(e) - S_1(e)]\times E_2\} \quad (13)$$

The tensile stress, which bark material withstands in the
For symmetrical cutter, N'_{21} is equal to N_{21}. So

$$T(\beta, e) = 2N_{21}(\beta, e)(\sin\frac{\beta}{2} + \mu\cdot\cos\frac{\beta}{2}) \quad (18)$$

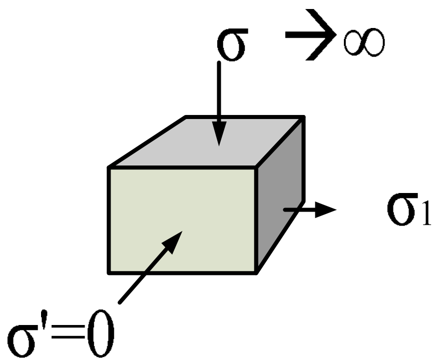

Figure 8. Stresses of core material.

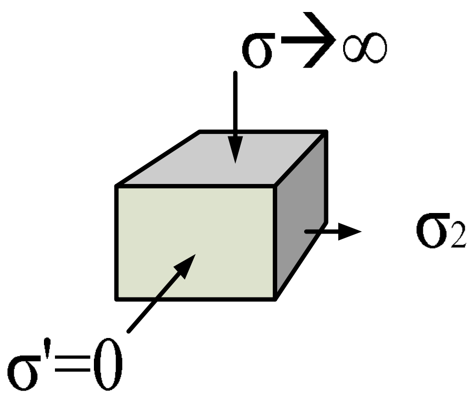

Figure 9. Stresses of bark material

$$\sigma_2 = \varepsilon \times E_2 \quad = 2P_1 \times E_2 / \{S_1(e) \times E_1 + [S(e) - S_1(e)] \times E_2\} \quad (14)$$

From Equation (4) we find that if $F > 0$ then $\sigma \to \infty$. Under the condition of $F > 0$, stresses at dangerous section are presented in Figures 8 and 9.

More also, when yielding occurs, the critical value of *F* is

$$F \approx [\sigma] \cdot (\bar{L} \times 2 \times r_\varepsilon) \quad (15)$$

Since $r_\varepsilon = 0$, from Equation (15) we find $F \to 0$ and $F > 0$. Thus;

$$\vec{T} + \vec{F}_{f_{21}} + \vec{N}_{f_{21}} + \vec{F}'_{f_{21}} + \vec{N}'_{f_{21}} \to 0$$

It means that the cutting force is mainly suffered by friction and by positive pressure. The cutting force can be expressed as;

$$\vec{T} = -(\vec{F}_{f_{21}} + \vec{N}_{f_{21}} + \vec{F}'_{f_{21}} + \vec{N}'_{f_{21}}) \quad (16)$$

Where,
$F_{f21}(\beta, e) = \mu \cdot N_{21}(\beta, e)$ and
$F'_{f21}(\beta, e) = \mu \cdot N'_{21}(\beta, e)$. μ is the friction coefficient between stalk mark and blade flank. Magnitude of cutting force is

fiber direction, is

$$T(\beta, e) = N_{21}(\beta, e)\sin\frac{\beta}{2} + \mu \cdot N_{21}(\beta, e)\cos\frac{\beta}{2} + N'_{21}(\beta, e)\sin\frac{\beta}{2} + \mu \cdot N'_{21}(\beta, e)\cos\frac{\beta}{2} \quad (17)$$

The area of cut mark is

$$s(e, \beta) = \frac{1}{\cos\frac{\beta}{2}}[\pi r^2 - S(e)] \quad (19)$$

Cut mark also has two parts: the core and the bark. In the cut mark region, the area of core is

$$s_1(e, \beta) = \frac{1}{\cos\frac{\beta}{2}}[\pi (r - \delta)^2 - S_1(e)] \quad (20)$$

While the area of bark is

$$s_2(e, \beta) = s(e, \beta) - s_1(e, \beta)$$

According to former assumptions, the material is anisotropy. The strength limit of core materials (η1) and bark materials (η2) are constant. Therefore;

$$N_{21}(e, \beta) = s_1(e, \beta)\eta_1 + s_2(e, \beta)\eta_2$$

Thus, Equation (18) can be expressed as

$$T(e, \beta) = [s_1(e, \beta)\eta_1 + s_2(e, \beta)\eta_2] \cdot (\sin\frac{\beta}{2} + \mu \cdot \cos\frac{\beta}{2}) \quad (21)$$

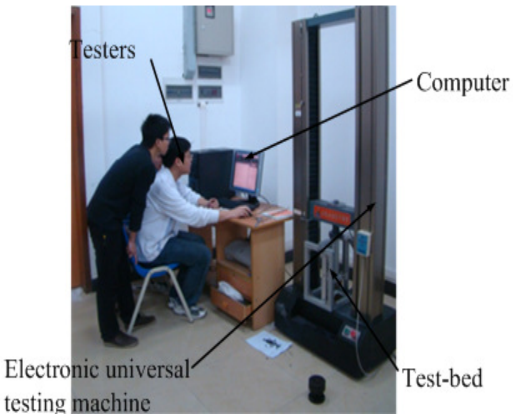

Figure 10. Test system.

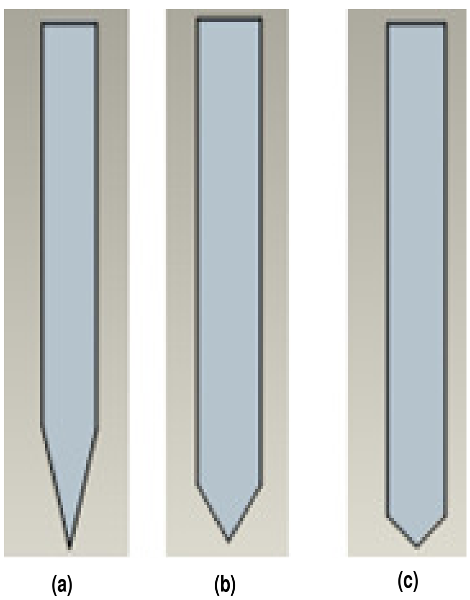

Figure 11. Testing cutters (a) β=.30°,(b) β=.60° and (c)β=.90°.

Equation (21) is therefore the model of cutting load.

EXPERIMENTAL VERIFICATION

Testing equipment

Photograph of the testing system is presented in Figure 10. The testing system includes a test-bed, an electronic universal testing machine and a computer. Test-bed was designed to reflect as closely as possible real cutting conditions in terms of both test and tool material.

Materials and methods

Test samples were stalks of Gui-Wei litchi which were harvested in April at Qingxi town, Dongguan, Guangdong, China. They were immediately transported to laboratory, and fruits and leaves on the stalk were removed by a sharp kitchen knife.

To evaluate influence of blade angle on cutting force, three pairs of V-cutters (Figure 11.), the blades' angle (β) of which in order was equal to 30°, 60°and 90°were selected as test cutters. The cutting velocity was 3.0 mm/min. During the tests, the centerline of test samples was perpendicular to cutter blade (cutting angle was equal to 90°). The acceptable error of blade angle and symmetry of blade flank were ± 0.5°. Cutters, whose blade angle was over the error, would be grinded by grinding wheel.

At the beginning of test, testers would grind the newly used cutter with a grinding wheel and then test sharpness and the error of blade angle and symmetry of blade flank. After each test was finished, testers would also test the sharpness of cutter blade. If they found that a cutter becomes slightly dull, they would then sharpen it by sandpaper. Sharpness was the only detecting item for those cutters which was sharpened by sandpaper. If there is gap on the blade of the cutter, testers would re-grind the cutter with a grinding wheel. Besides sharpness, blade angle and its symmetry were the other two detecting items for those cutters which were re-grinded by grinding wheel. Obviously, sharpness detection is an important step in each test, and this was detected by comparing with sharp knives.

Results and discussion

All calculated results were based on the hypothesis that friction coefficient is 0.4. The value of strength limit was obtained by pulling similar simples; strength limit of bark material is supposed to be equal to 1/10 of that of core material. The cutting force trend-line calculated by Equation (21) was very similar to test results, but the calculated trend-line was much smoother. The difference might have resulted from radial anisotropy of test samples. Figure 12a is an example of simulated curve of cutting force by Equation (21), while Figure 12b is an example of recorded test result.

Figures 13 to 15 are calculated and tested max force of cutting samples by cutters of β = 30°, 60°and 90°. No matter how much β is, when radius is around 4 and 3 mm, the average of test results is less than calculated results by Equation (21), and if radius of sample is around 7, 8 and 9 mm, the average of test results is bigger than calculated results. It was observed that the smaller the radius of samples, the less its strength limit; while the bigger the radius of samples, the more its strength limit.

Such differences might be resulted from mechanical properties difference between samples. Although, when radius of sample is between 5 and 7 mm, the calculated results were not absolutely equal to test results, but were very approximate to their average. Additionally, both experimental results and calculated results demonstrated that max cutting force increases with blade angle.

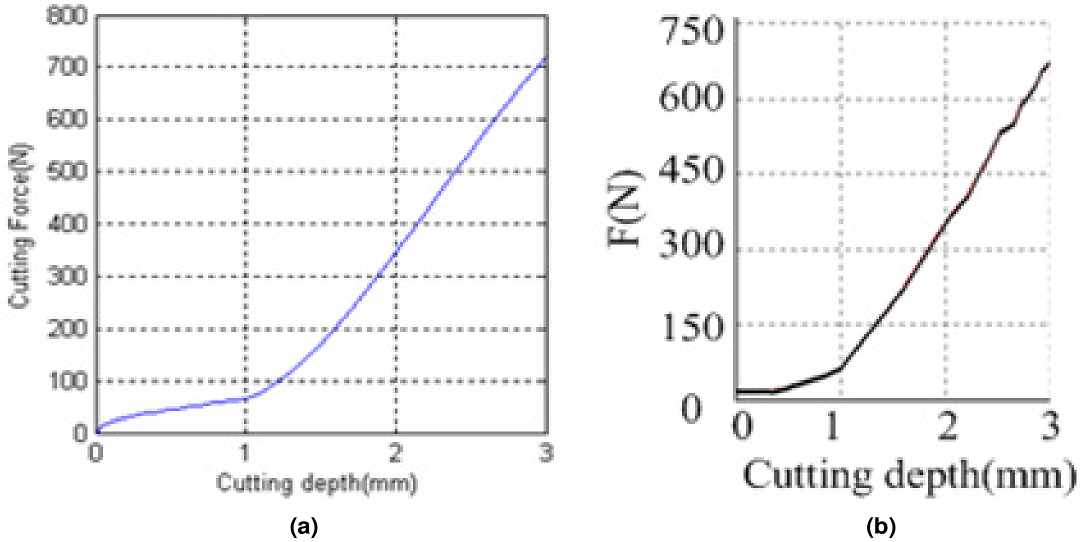

Figure 12. (a) A simulated curve and (b) a test result.

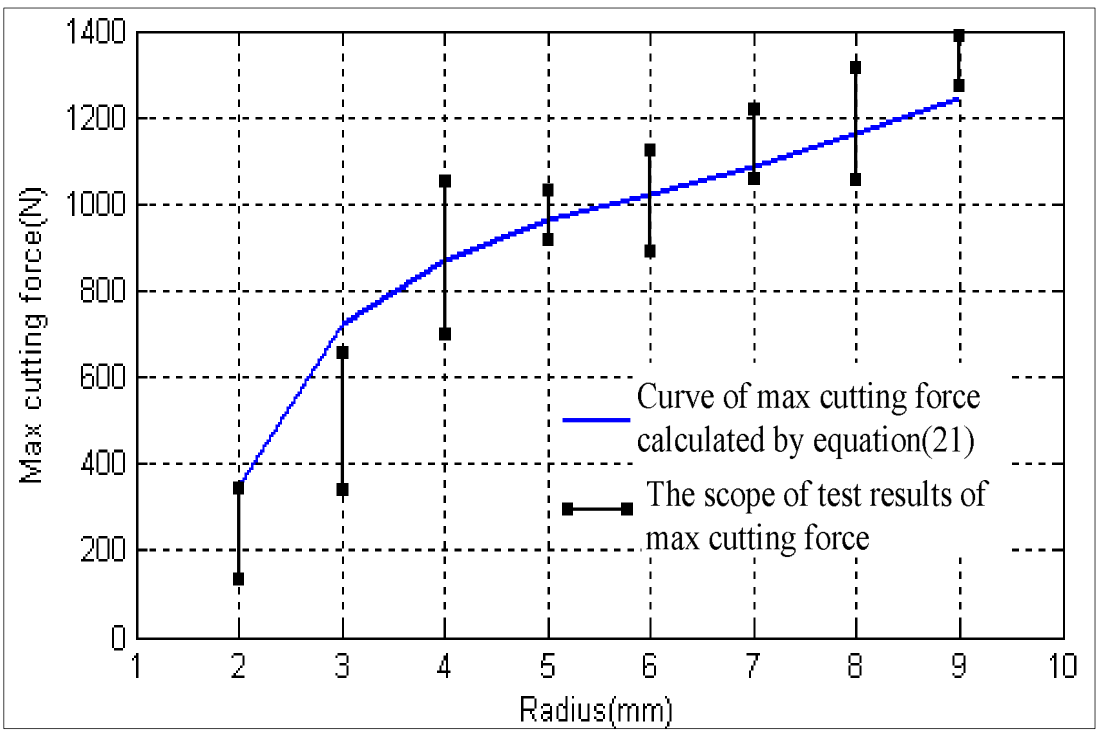

Figure 13. Max cutting force(β=.30°).

CONCLUSION

In this paper, a model describing the relationship among cutting load, blade angle and friction coefficient was developed for cutting operation with sharp V-cutter. A testing-equipment was developed and a series of tests was designed to verify such model. Results indicated that the cutting force trend-line calculated by the model was very similar to test results, but the calculated trend-line is much smoother. Also, when radius of sample was between 5 and 7 mm, the calculated results were very approximate to the average of test results. Both calculated

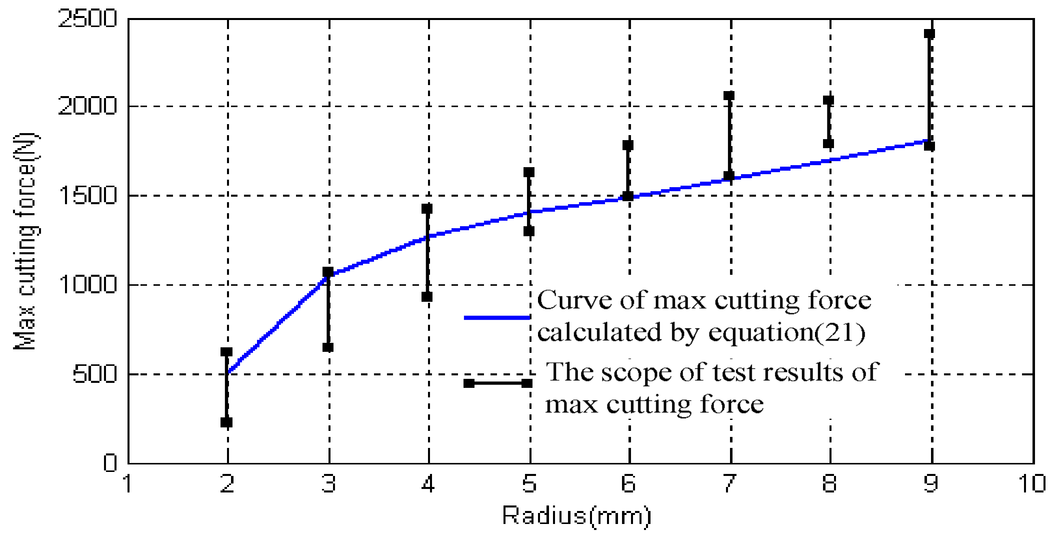

Figure 14. Max cutting force(β= 60°).

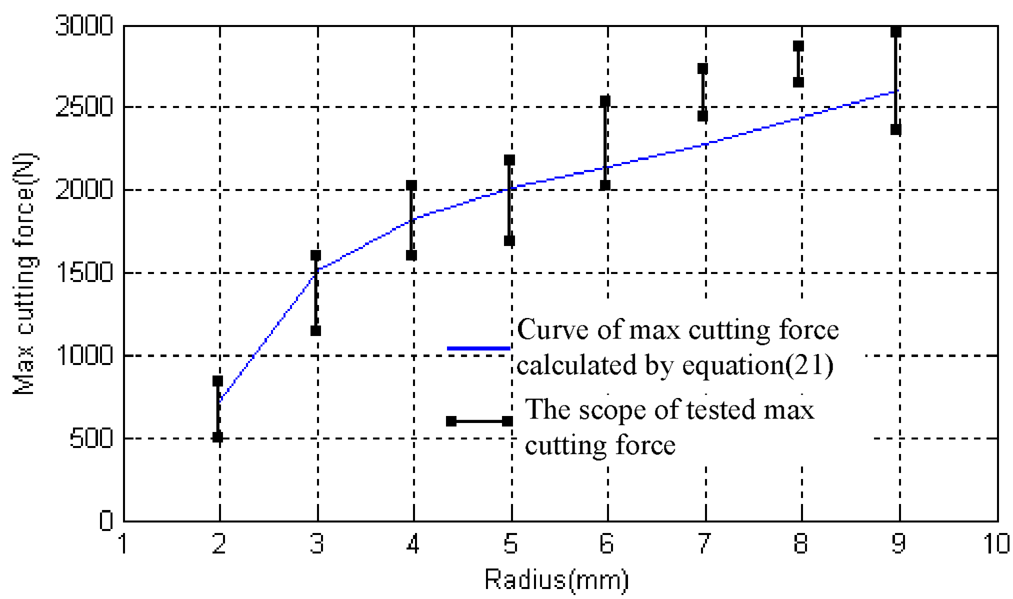

Figure 15. Max cutting force(β = 90°).

results and experimental results therefore indicated that the max cutting force increases with blade angle.

ACKNOWLEDGEMENTS

The research work of this paper is jointly supported by National Science Project of China with Research Grant 30900870 , 50775079 and 51005080 , Talent Foundation of Guangdong Province Colleges and universities with Research Grant[2010]-79, Science Project of Guangdong Province with Research Grant S2011010001933.

REFERENCES

Deniz Y, Onder K, Ibrahim A, Aziz O, Ilhan C M (2009). Effect of moisture content and stalk section on some engineering company parameters of closed capsule sesame stalks (Sesamum indicum L.). J. Food, Agric. Environ.Vol.7 (3&4) : 306-311.

El Hag H E, Kunze O R, Wilkes L H (1971). Influence of moisture, dry-matter density and rate of loading on ultimate strength of cotton stalks. Trans. ASABE 13(3): 713 -716.

Esehaghbeygi A, Hoseinzadeh B, Khazaei M, Masoumi A (2009). Bending and Shearing Properties of Wheat Stem of Alvand Variety. World Appl. Sci. J. 6 (8): 1028-1032.

Galedar MN, Jafari A, Mohtasebi SS, Tabatabaeefar A, Sharifi A, O'Dogherty MJ, Rafiee S, Richard G (2008). Effect of moisture

Majumdar content and level in the crop on the engineering properties of alfalfa stems. Biosys. Eng. 101: 199-208.
Khazaei J, Rabani H, Ebadi A, Golbabaei F (2002). Determining the shear strength and picking force of pyrethrum flower. AIC Paper No. 02-221, Canadian Society of Association Executives (CSAE), Mansonville, Que. Canada.
Kocabiyik H, Kayisoglu B (2004). Determination of shearing features of sunflower stalk. J. Agric. Sci. 10(3): 263-267
Liu Q, Ou Y, Qing S, Song O (2007). Cutting force test of sugarcane stalk. Transactions of the Chinese Soc. Agric. 23(7): 90-94
Majumdar Dutta RK (1982). Impact cutting energy of paddy and wheat by a pendulum type dynamic test. J. of Agric. Eng. Res. 19(4): 258-264.
Mesquita C M. Hanna M A (1995). Physical and mechanical properties of soybean crops. Trans. ASABE 38(6): 1655-1658
Murray R S (1982). Theory and problems of theoretical mechanics. McGRAW-HILL book
Persson S (1987). Mechanics of Cutting Plant Material. ASAE Publications, Michigan.
Razak J (1997). Design and development of an oil palm fresh fruit bunch cutting device. M. SC thesis. Universiti Putra Malaysia.
Tabatabaekoloor R. (2008). Effect of blade angles and velocities on the cutting energy of paddy stem. Agricultural and biosystems engineering for a sustainable world. International Conference on Agricultural Engineering, Hersonissos, Crete, Greece, 23-25 June, 2008. OP-1930. 4 ref
Xiao Z, Liu S, Hu Y (2000). Wood cutting tools Techology. Northeast Forestry University Press.7 (In Chinese).
Yiljep YD, Mohammed US (2005). Effect of Knife Velocity on Cutting Energy and Efficiency during Impact Cutting of Sorghum Stalk. Agricultural Engineering International: the CIGR E .J. Manuscript PM 05 004. Vol. VII.